Polymer 51 (2010) 2494–2502

Contents lists available at ScienceDirect

Polymer

journal homepage: www.elsevier.com/locate/polymer

Synthesis and characterization of transparent alumina reinforced polycarbonate nanocomposite

Hamid R. Hakimelahi, Ling Hu, Bradley B. Rupp, Maria R. Coleman*

Department of Chemical & Environmental Engineering, University of Toledo, 2801 West Bancroft Street, Ohio 43606-3390, USA

ARTICLE INFO

Article history:
Received 3 November 2009
Received in revised form
4 April 2010
Accepted 10 April 2010
Available online 18 April 2010

Keywords:
Polycarbonate nanocomposite
Alumina nanowhisker
In-situ polymerization

ABSTRACT

Transparent nanocomposite films were fabricated by blending a concentrated nanocomposite formed by in-situ polymerization of polycarbonate in the presence of alumina nanowhisker with a high molecular weight polycarbonate. Polycarbonate was grafted to the alumina nanowhisker surface to improve nanofiller dispersion and load transfer to polymer matrix. Fourier transform infrared spectroscopy confirmed the functionalization of the nanowhisker with polycarbonate. Samples produced using functionalized alumina exhibited improved dispersion compared to the raw alumina nanowhiskers in the PC. Functionalization of alumina nanowhisker enhanced tensile properties (Young's modulus and tensile strength) relative to the pure polycarbonate and blends produced with raw alumina nanowhisker. Additionally, the nanocomposite formed using in-situ polymerization showed small decreases in transparency in the visual range compared to the base polymer with increased absorption in the UV range. The effect of reaction temperature during in-situ polymerization on the properties of the nanocomposite was investigated. Higher reaction temperature resulted in improved dispersion and sharp increases in tensile modulus and shear strength.

1. Introduction

Polycarbonate (PC) is a commercially important engineering thermoplastic that possesses several distinct properties including transparency, dimensional stability, flame resistance, high heat distortion temperature, high impact strength and moisture insensitivity [1–6]. It can be widely used in applications that require transparency and impact resistance including windshields, canopies, vision blocks, face shields, goggles and lenses [7]. There is considerable interest in improving the mechanical properties of PCs while maintaining transparency. Several approaches have been investigated to improve the mechanical performance of PC including the addition of small amounts of core-shell impact modifier [8], short glass fiber [9,10], inorganic whiskers such as aluminum borate whiskers [3], potassium titanate whiskers [2], carbon nanotube or nanofiber [11–16], polyhedral oligomeric silsequioxane (POSS) [17], organoclay [18–21], atomic layer deposited alumina films on PC substrate [22] or polycarbonate layered-silicate nanocomposite [23]. Researchers saw improved tensile properties but often at expense of transparency [24–26].

In order to obtain a transparent composite film, the particle size of the filler should be less than half of the shortest wavelength of visible light (380–570 nm) to minimize scattering at the interface between the filler and polymer matrix [27,28]. Therefore, nanofillers are ideal choices for reinforcement of transparent polycarbonate composite. Since intrinsically poor compatibility of most inorganic nanofillers with polymer matrix leads to poor dispersion and aggregation of nanofillers in polymer matrix, polymer nanocomposite films are typically not transparent even at very low loadings [24–26]. Therefore, good dispersion of nanofiller in the polymer matrix is essential to fabrication of transparent polymer nanocomposites. Also, sensitivity of PC to impurities in nanofillers during processing which results in color formation is another issue in making transparent PC-based nanocomposites [18,19].

Little success has been reported for PC nanocomposites that exhibit improved mechanical properties without considerable loss in transparency. For example Hanemann and Haubelt [26] produced polycarbonate–alumina-composites using compounding and micro injection molding. They reported a small change in mechanical strength of the composite compared to the pure polymer while optical transmittance dropped significantly when particles were added. This was attributed to the nanoparticles agglomeration in the films. Also, Yoon et al. [18,19] prepared PC nanocomposites using melt processing from a series of organoclays

* Corresponding author. Tel.: +1 419 530 8091; fax: +1 419 530 8086.
E-mail address: maria.coleman6@utoledo.edu (M.R. Coleman).

0032-3861/$ – see front matter © 2010 Elsevier Ltd. All rights reserved.
doi:10.1016/j.polymer.2010.04.023

based on sodium montmorillonite exchanged with various amine surfactants. While there was an increase in modulus and tensile stress of these composites relative to PC, there was a color formation due to the use of organoclay and its structure during melt processing. They found that the extruder with the longer residence time and broader residence time distribution was more effective for dispersing the clay but gave more color. Also, double bond in the surfactant leads to more color depth than saturated surfactants and more severe color was observed in the surfactants containing both hydroxyl-ethyl groups and tallow tails. Therefore, design of a transparent nanocomposite with improved mechanical properties requires consideration of nanofiller properties, purity of polymer and nanofiller, processing methods and improving load transfer between polymer and nanofiller.

Inorganic whiskers are of great interest as reinforcement for nanocomposites because they exhibit high stiffness and strength. Since whiskers are nearly free from internal flaws due to their small diameter, their yield strength tends to approach the maximum theoretical value expected from the theory of elasticity [29]. Silicon carbide, potassium titanate and aluminum borate whiskers have been used as nanofillers; however, their large sizes (500–1000 nm in diameter and 5–40 μm in length) would not allow formation of transparent polymer composites [2,3]. Alumina nanowhiskers were chosen as the reinforcing nanofiller in this study because they are transparent, commercially available, have high strength and large concentration of surface reactive hydroxyl groups that are available for subsequent functionalization [30,31].

Surface functionalization with targeted groups can be used to compatibilize inorganic fillers within polymer matrices and improve dispersion in solvents [32]. Several approaches have been used to modify the surface functionality of nanofillers including covalent binding of compatibilizing groups, wrapping with polymer chains, blending with surfactants and in-situ polymerization in presence of nanofillers [2,14, 18, 19, 24,32–36]. These methods have been used with varying success to produce composites with dispersed nanofillers. This paper focuses on a combination of in-situ polymerization and blending to produce composites of modified alumina nanowhisker in polycarbonate.

Tensile properties and optical transparency were investigated for polycarbonate composite films with loadings of alumina nanowhisker up to 2 wt%. Scanning electron microscopy (SEM) was used to observe dispersion of alumina nanowhisker in the fracture surface of polycarbonate composite films. The impact of polymerization temperature and nanowhisker loading on tensile properties will be discussed.

2. Experimental section

2.1. Materials

Aluminum oxide nanowhisker with diameter of 2–4 nm, length of 2800 nm and surface area of 350–720 m^2/g were purchased from Sigma-Aldrich (Milwaukee, WI). The high molecular weight polycarbonate (referred to base PC) used for diluting nanocomposite master batch and for the plain polycarbonate films was purchased from Sigma-Aldrich with a molecular weight of approximately 64,000. Bisphenol A and triphosgene were the monomers used for in-situ polymerization, while pyridine was used as a solvent, triethylamine (Et_3N) as a catalyst, and methanol as a precipitant. Methylene chloride was the solvent used in the solution casting process. All chemical reagents were purchased from Sigma-Aldrich and used without further purification. Extruded plain PC films were bought from McMaster-Carr (Cleveland, OH) with a thickness between 0.12 and 0.14 mm to test the optical transmittance relative to the solution cast films.

2.2. In-situ polymerization

The technique used for in-situ polymerization of PC in the presence of the alumina nanowhisker is similar to the method utilized by Wang et al. [37,38] to copolymerize PC with poly (ρ-ethylphenol). The method used to synthesize a master batch outlined below:

A mixture of 5.1 mmol (1.16 g) bisphenol A was dissolved in 15 ml of pyridine along with 2.6 mmol (0.26 g) alumina nanowhisker in a flat-bottom flask. After sonication for 30 min at room temperature (Ultrasonic cleaner, Model FS60, Fisher Scientific, Pittsburgh, PA), 1.7 mmol (0.50 g) of triphosgene was added to the solution. Finally, 5.1 mmol (0.7 ml) of triethylamine was added dropwise to the mixture under agitation and the reaction temperature was set. After 24 h, the reaction mixture was poured into a large excess of methanol to precipitate the PC nanocomposites. The precipitated composite master batch powder was washed with methanol several times and dried in a vacuum oven at 100 °C for 48 h.

2.3. Solution casting of films

The nanocomposite master batch was diluted with high molecular weight PC, which is referred to as base PC, to produce composites with desired concentration of alumina nanowhisker. For each composite film, 1.4–1.7 g of base PC (depending on the fiber loading) was blended with the 0–0.3 g of the nanocomposite master batch and dissolved in 15–17 ml of methylene chloride. The solution was sonicated at room temperature for 30 min, mixed for at least 12 h, and finally cast in a clean glass dish in a hood for 24 h to form freestanding film. For the plain polycarbonate film, 1.7 g of base PC was dissolved in 15–17 ml of methylene chloride. The resulting films were dried under vacuum at 160 °C overnight to remove residual solvent prior to characterization. The designation for the resulting composite films is PC-Al_2O_3-reaction temperature-loading. For example PC-Al_2O_3-RT-2% refers to the nanocomposite master batch of room temperature synthesis which was diluted with base PC to produce a composite with nanowhisker loading of 2 wt%. The relative mass of master batch and base PC required to produce a desired alumina nanowhisker loading was determined using an estimated alumina concentration in the synthesized master batches as shown in Table 1. These alumina loadings were estimated from an assumption of no loss of alumina during in-situ polymerization for each master batch.

A 2 wt% composite was also produced by blending the base PC with raw alumina nanowhisker. In this case, the 0.034 g of raw alumina nanowhisker was sonicated with 1.666 g base PC in 15–17 ml of methylene chloride, and cast in a clean glass dish using a process similar to the nanocomposite films as described earlier. The composite produced using blending is designated as PC-R-Al_2O_3-2%.

2.4. Characterization

Gel permeation chromatography (GPC) was carried out on a SCL-10Avp Shimadzu high-performance liquid chromatograph

Table 1
Relative masses of master batch and base PC required producing approximately 0.5% loading nanocomposite.

Sample name	Alumina concentration in master batch (%)	Master batch (gr)	Base PC weight (gr)
PC-Al_2O_3-RT-0.5%	20.7	0.0411	1.6589
PC-Al_2O_3-44-0.5%	16.1	0.0527	1.6473
PC-Al_2O_3-55-0.5%	14.2	0.0600	1.6400

(Columbia, MD) to obtain the molecular weight distribution (MW). The eluent was HPLC methylene chloride and the column operated under flow rate of 1 ml/min. A calibration plot, constructed with polystyrene standards in the range of 980–500,000, was used to determine the molecular weights.

Fourier transform infrared (FTIR) spectra of raw alumina nanowhisker and the nanocomposite master batch synthesized at room temperature were recorded on a DigiLab FTS 400 spectrophotometer (Holliston, MA) using KBr pellets. FTIR was used to verify the structure of the polycarbonate extracted from the master batch and any groups that were covalently bound to the nanofiller surface. Soxhlet extraction was used to isolate the unbound PC from the alumina nanowhisker. For this experiment, the unbound PC was extracted from the in-situ polymerized PC with THF for 24 h [32]. FTIR spectra for residue nanowhisker were recorded using KBr pellets.

The temperature dependent dynamic mechanical properties of the PC-Al_2O_3-RT films were measured using a TA Instruments Q800 (New Castle, DE) series dynamic mechanical analyzer (DMA) in tensile mode at an oscillation frequency of 1.0 Hz. DMA data was collected from room temperature to 170 °C at a heating rate of 2 °C/min.

Tensile tests were performed on Model 5560 Instron tensile machine (USA) according to ASTM D-638-5 with a cross-head speed of 1 mm/min at room temperature. Specimens were cut in a dog bone shape using a cutting die as specified in ASTM D-638-5. The length and width of each specimen was 25.05 and 3.18 mm, respectively. The thickness varied from 0.09 to 0.11 mm.

The optical transmittance of the PC and alumina reinforced PC nanocomposite films were monitored using a Cary 5 Diode Array UV–vis–NIR spectrophotometer (HP8452). The total light transmittance of each film was monitored over a wavelength range from 300 to 1000 nm for films of thickness 0.15–0.16 mm.

Hitachi S-4800 High Resolution Scanning Electron Microscope (SEM) was used to investigate the morphology of the fracture surface of the PC composite. All samples were fractured during tensile testing to observe both alumina nanowhisker dispersion and pull out. The samples were coated with a thin gold layer for further observation.

3. Result and discussions

3.1. In-situ polymerization

Polycarbonate-alumina nanowhiskers composites were produced using an in-situ polymerization blending approach. This method consisted of synthesis of polycarbonate in the presence of alumina nanowhiskers to form a concentrated master batch. The concentrated nanocomposite master batch will be referred to as MB-T in which *T* is the reaction temperature. For example, the master batch nanocomposite synthesized at 55 °C is MB-55. The master batch was blended with a high molecular weight PC to form the composite films used for property testing. In addition, pure PC was synthesized using this method to allow for comparison of the chemical structure and molecular weight distribution and designated as PC-T in which *T* is the reaction temperature.

A modified reaction procedure with bisphenol A and triphosgene was used for in-situ polymerization to allow for both bulk polycarbonate synthesis and reaction between the free hydroxyl groups of alumina nanowhisker and triphosgene [37,38]. This can result in the formation of two independent populations of PC during polymerization: (i) bulk polycarbonate and (ii) PC that is covalently bound to the nanowhisker surface as illustrated in Fig. 1.

The yield and estimated concentration of alumina in nanocomposite master batch (MB-T) were calculated using the following equations:

$$\text{Yield}(\%) = \frac{\text{Product}(g)}{\text{Total monomers}(g)\text{and } Al_2O_3} \times 100 \quad (1)$$

$$\text{Alumina Concentration}(\%) = \frac{\text{Initial amount of alumina used in in-situ polymerization}(g)}{\text{Amount of MB-T}(g)} \times 100 \quad (2)$$

A key assumption is that no alumina nanowhiskers were lost during polymerization and product recovery. These estimated values for alumina concentration were used to determine the relative amounts of master batch and pure PC required to produce each of the nanocomposites.

In order to confirm the estimated alumina concentrations, Soxhlet extraction with THF for 24 h was used to isolate bulk

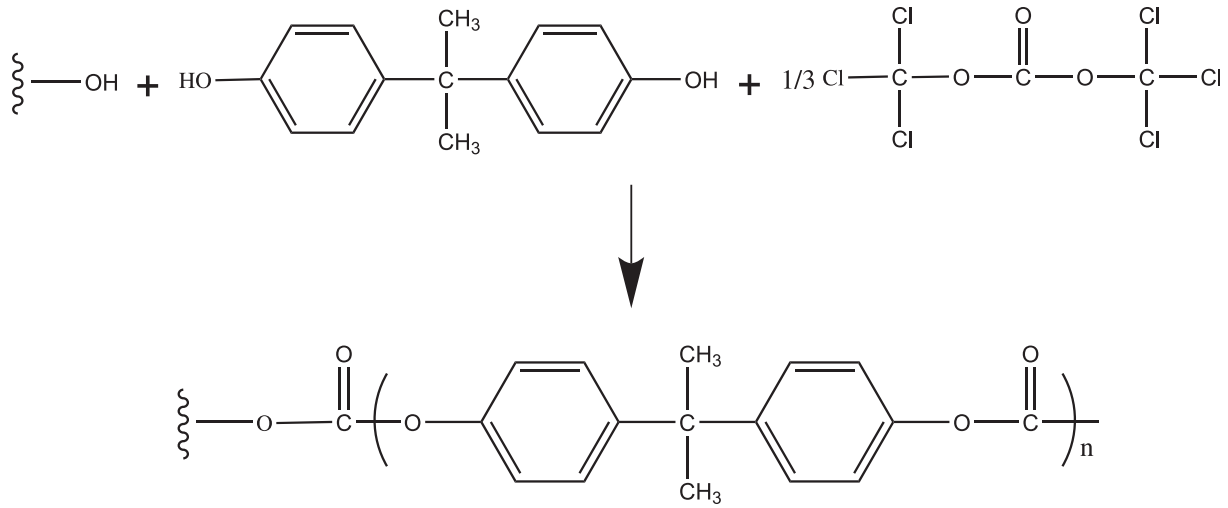

Fig. 1. Proposed reaction chemistry of in-situ polymerization to grow polycarbonate oligomer on the alumina nanowhisker surface (The reaction for bulk polycarbonate is similar to the surface reaction).

polycarbonate and alumina nanowhiskers from the master batches synthesized at room temperature, 40 and 55 °C. The mass of the master batch extracted bulk PC and functionalized alumina nanowhiskers were measured and used to determine the concentration of alumina in each master batch as shown in Table 2. Besides, the molecular weight of each was measured by using GPC to investigate the effect of temperature on PC chain growth. The yield of reaction and molecular weight for pure PC synthesized at room temperature, 40 and 55 °C is also reported in Table 2.

The yield and molecular weight for the pure PC and the bulk PC recovered from master batches increased with increasing reaction temperature. The concentrations of alumina nanowhiskers in the master batches monitored using extraction of components from the master batch were within 10% of values estimated based on Eq. (2).

3.2. Chemical structure of master batch

In-situ polymerization involved formation of polycarbonate in the presence of alumina nanowhisker using standard polymerization reactions. During in-situ polymerization the alumina nanowhiskers were dispersed in polycarbonate. In addition, polycarbonate chain can be covalently bound to the surface through reaction with the hydroxyl group on the surface of the alumina nanowhisker.

FTIR analysis was used to confirm the structure of the bulk polycarbonate and the presence of groups covalently bound to the surface of alumina nanowhisker following in-situ polymerization. Specifically, the FTIR spectra for pure PC synthesized using the same method as in-situ polymerization, the PC oligomer recovered from the master batch, raw alumina nanowhisker and the functionalized alumina nanowhisker are compared in Fig. 2(a) and (b). The FTIR spectra for (A) pure PC and (B) PC oligomer recovered from the MB-RT are compared in Fig. 2(a).

Characteristic transmittance peaks for the components of the polycarbonate, raw and functionalized alumina nanowhisker at different reaction temperatures are shown in Table 3. The peaks for pure PC are consistent with literature reports [37,38]. The polycarbonate oligomer recovered following Soxhlet extraction of the MB-RT exhibited characteristic peaks that were similar to those of the pure PC. For example, the characteristic peak at 1772 due to the carbonyl C=O stretch as well as peaks corresponding to aliphatic CH stretch around 2970 are present in both spectra. A transmittance peak around 3400 cm^{-1} that can be attributed to OH stretching mode occurs in the spectrum of pure PC and recovered PC oligomer. This shows that both PC are hydroxyl end-capped which is consistent with the low molecular weight of the synthesized PC.

The FTIR spectra for the functionalized alumina nanowhisker obtained by Soxhlet extraction of the master batches and raw alumina nanowhisker are shown in Fig. 2(b). The sharp peak around 3400 cm^{-1} is attributed to the OH stretching mode of the hydroxyl groups on the surface of the raw alumina. This result is consistent with the data reported by Bin Gu and Ayusman Sen [31]. As shown in Fig. 2(b) and Table 3, several new peaks are present in

Table 2
Polymer yield of polymerization and alumina concentration of the master batch and pure PC produced at different reaction temperatures.

Composite	Yield (%)	MW	Estimated Alumina Concentration (%)[a]	Measured Alumina Concentration (%)[b]
MB-RT	65.8	9,044	20.7	22.3
MB-40	84.4	14,020	16.1	19.2
MB-55	96.1	16,296	14.2	16.1
PC-RT	70.5	11,781	–	–
PC-40	89.2	16,694	–	–
PC-55	98.4	19,918	–	–

[a] Estimated by Eq. (2).
[b] Obtained by Soxhlet extraction.

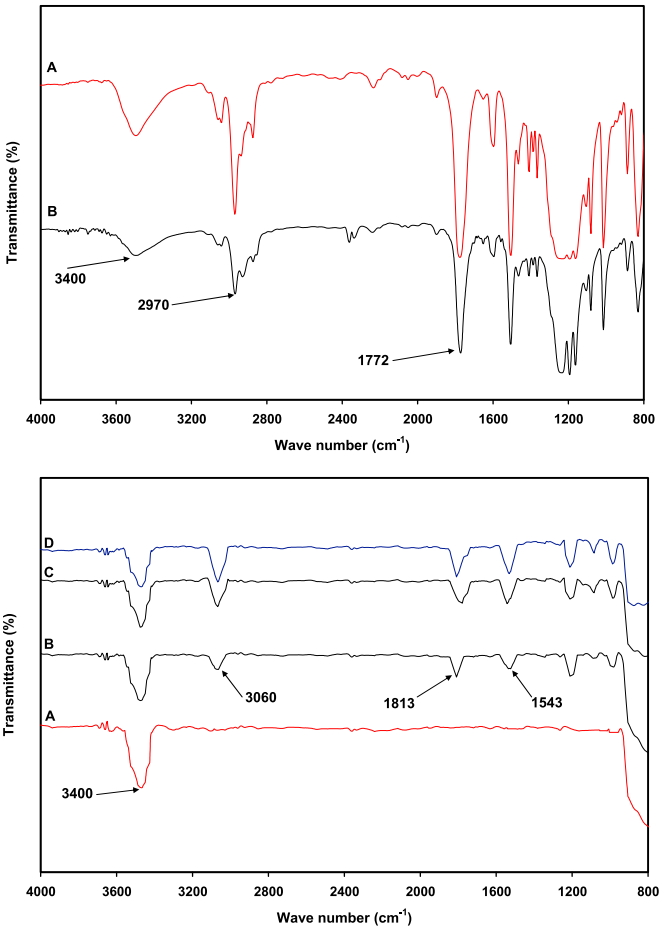

Fig. 2. (a) FTIR spectra of (A) pure polycarbonate synthesized using the procedure for in-situ polymerization and (B) polycarbonate oligomer recovered from the master batch. (b) FTIR spectra of (A) raw alumina nanowhisker (B) functionalized alumina nanowhisker isolated from MB-RT (C) functionalized alumina nanowhisker isolated from MB-40 and (D) functionalized alumina nanowhisker isolated from MB-55.

the spectrum of the functionalized alumina nanowhisker. For instance, a peak occurs at 3060 cm^{-1} that is consistent with aromatic stretching peaks. A peak at 1813 cm^{-1} is due to C=O stretching and peak around 1543 cm^{-1} is attributed to aromatic ring stretching. These peaks are consistent with the characteristic peaks of the unbound PC oligomer that was recovered following Soxhlet extraction as shown in Fig. 2(a). All the functionalized alumina nanowhiskers were thoroughly washed so that these peaks can be attributed to the PC grafted to the alumina nanowhiskers [32]. Zhong Zeng, et al. [30] reported similar results for polystyrene/alumina composite nanoparticles produced through emulsion polymerization in the presence of the alumina. The relative intensity of the peak at 3400 cm^{-1} assigned to (Al)-OH for the functionalized nanowhiskers is smaller than that for the raw alumina nanowhisker. This indicates that not all of the hydroxyl groups on the surface of alumina nanowhiskers participated in in-situ polymerization, which is similar to the observation for alumina/PMMA-co-PBA composites by Bin Gu, et al [31].

Interestingly, the intensity of peaks corresponding to the grafted PC oligomer increases with increasing the reaction temperature for the master batch. The intensity of OH stretching peak decreases at high reaction temperatures which may be due to increased participation by surface hydroxyl groups of nanowhiskers in binding of PC. These results are consistent with increasing concentration of backbone groups of PC bound to the alumina nanowhiskers at higher reaction

Table 3
Characteristic absorbance bands for pure polycarbonate, polycarbonate oligomer with OH end cap, raw alumina nanowhisker and functionalized alumina nanowhisker in the range of 400–4000 cm^{-1}. The pure PC and nanocomposite were synthesized at room temperature.

Band assignment	Pure PC (cm^{-1})	PC oligomer (cm^{-1})	Raw alumina (cm^{-1})	Functionalized alumina at different reaction temperatures (cm^{-1})
OH stretching	3400	3400	3400	3400
Aromatic CH stretching	3060	3060		3060
Aliphatic CH stretching (CH_2 and CH_3)	2970	2970		
	2935	2935		
C = O stretching	1786	1786		1813
Aromatic ring stretching	1612	1612		1543
	1508	1508		
C–O–C stretching (γ_{as} & γ_s)	1265–1100	1265–1100		1211
Aromatic CH in-plane bending	1080 & 1014	1080 & 1014		1091
Aromatic CH out of plane bending	889	889		987
	831	831		

temperatures, which can be attributed to presence of longer polycarbonate chains and/or higher concentration of bound PC chains.

3.3. Room temperature nanocomposites

3.3.1. Thermal-mechanical properties of RT nanocomposites

3.3.1.1. Dynamic mechanical testing. The thermal-mechanical properties of nanocomposites based on the diluted MB-RT were characterized using dynamic mechanical analysis and Instron tensile testing. These samples were compared with a composite produced by blending raw alumina with the high molecular weight polycarbonate at 2 wt%. Dynamic mechanical analysis was used to investigate the impact of alumina nanowhisker loading and processing method on chain mobility (T_g) and bulk stiffness (storage modulus) of the polycarbonate nanocomposites.

The storage modulus (G′) at different loadings of alumina nanowhisker, which measures the energy stored during deformation and is related to the solid-like or plastic portion of the polymer, is plotted as a function of temperature in Fig. 3. This figure compares the storage modulus for plain PC with those of PC-Al_2O_3-RT composites produced using blending and in-situ polymerization/blending. The storage modulus represents the stiffness of the sample and shows the properties of glassy state (high modulus) at low temperatures and rubbery state (low modulus) at high temperatures. All of the in-situ polymerization/blending based composites exhibited increases in storage modulus relative to plain PC at temperatures below 110 °C. For example, as the estimated loading of alumina nanowhisker was increased from 0 to 2.3%, the storage modulus at 60 °C increased from 1930 to 2555 MPa (Fig. 3). There was only a small change for the in storage modulus for composite with raw alumina nanowhisker (from 1930 to 2023 MPa). Therefore, the composite became stiffer for samples produced using in-situ polymerization/blending, while blending with raw alumina had little effect on stiffness.

The location of the tan δ peak versus temperature for the plain PC and PC-Al_2O_3-RT composites at 1 Hz are shown in Fig. 4. The tan δ peak of the composite based on in-situ polymerization/blending became broader and shifted to lower temperatures with increasing loading of alumina. In fact, all of the in-situ based PC composites exhibited lower T_gs with increasing loading of alumina. However, the PC-R-Al_2O_3-2% composite exhibited similar T_g to that of the plain PC. At loading of 1.6% or greater for PC-Al_2O_3-RT based composites, a low temperature shoulder appeared to the T_g peak. This shoulder peak may be due to the presence of low molecular weight polycarbonate oligomer both in bulk and/or bound to the nanowhisker surface. This would become increasingly important as the ratio of the master batch to bulk PC was increased; the low molecular weight PC had a large contribution to the overall properties of the PC-Al_2O_3-RT composite.

Dynamic mechanical testing shows that the inclusion of functionalized alumina nanowhisker with the Young's modulus around 530 GPa (from technical datasheet provided by Sigma-Aldrich for alumina nanowhiskers) results in a general increase in stiffness of the polymer matrices as indicated by the storage modulus. Interestingly, there is a corresponding decrease in glass transition temperature that is consistent with increasing concentration of low molecular weight PCs in the composite.

3.3.1.2. Tensile testing. Tensile testing of the polycarbonate composites was performed as a function of weight percentage of alumina nanowhisker for comparison with dynamic mechanical

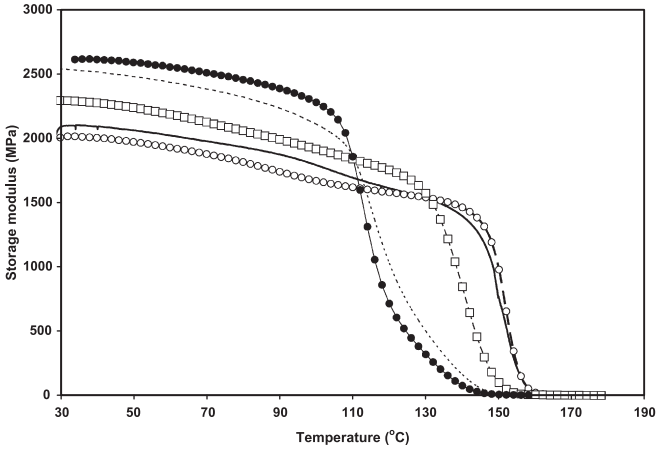

Fig. 3. Storage modulus versus temperature for (○) plain PC, (_) PC-R-Al_2O_3-2 wt%, (□) PC-Al_2O_3-RT-1 wt%, (…) PC-Al_2O_3-RT-1.6 wt%, (●) PC-Al_2O_3-RT-2.3 wt%.

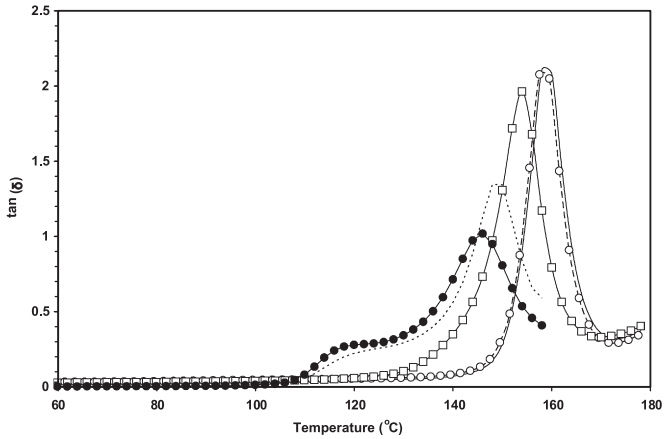

Fig. 4. Tan δ curve in glassy state region for (_) plain PC, (○) PC-R-Al_2O_3-2 wt%, (□) PC-Al_2O_3-RT-1 wt%, (…) PC-Al_2O_3-RT-1.6 wt%, (●) PC-Al_2O_3-RT-2.3 wt%.

analysis. The presence of bound polycarbonate chains on the surface of alumina nanowhisker was expected to improve the chemical and physical interactions at the fiber-matrix interface that can translate to improvement in load transfer at the interface. Additionally, wrapping of the nanowhiskers by growing PC chains during in-situ polymerization could contribute to improved dispersion and tensile properties [39–41].

The impact of surface functionalization on the tensile properties of the solution cast PC nanocomposites is demonstrated for the tensile stress–strain curves for 0.5 wt% fiber loading shown in Fig. 5. Plain PC exhibits a typical shape for stress–strain curve with a yield tensile strength of 30 MPa and yield strain of 3%. Also, a neck formed for plain PC which indicates relatively large amounts of strain localized disproportionately in a small region of the PC [42]. When 0.5 wt% raw alumina fiber was blended with the base PC, the material became more brittle and broke at lower strain of about 2.4% with little change in tensile stress at yield (around 33 MPa).

In-situ polymerized/blended composite at low loading (i.e. PC-Al_2O_3-RT-0.5%) exhibited an increase in tensile yield strength with little change in the strain at yield relative to plain PC. The PC-Al_2O_3-RT-0.5% exhibited similar strain at yield and necking as the plain PC but higher strength. At loading of 1 wt% and higher no necking was observed, which indicates the composite becomes more brittle at higher loadings (not shown in Fig. 5). Even at low loading (0.5 wt %) the presence of bound polycarbonate on the surface of alumina appears to improve the interfacial interaction and load transfer between the fibers with the matrix. This led to improved strength without much loss in strain at yield. The results for higher temperature synthesis will be discussed in detail in a later section.

The impact of nanowhisker loading for the samples produced by blending the base PC with the MB-RT on the Young's modulus is compared to results for raw alumina blending approach in Fig. 6. The yield tensile strengths at room temperature are plotted as function of nanowhisker loading in Fig. 7. In all cases, three samples each of four specimens were tested and average values are reported. There was an increase in both the Young's modulus and the tensile strength with increasing loading for the PC-Al_2O_3-RT composite. For example, the Young's modulus increased from about 2230 MPa for plain PC to 2680 MPa for 2% loading with corresponding increase in tensile strength from 32 to 56 MPa. The strain did not change significantly over this concentration range (with values between 2.7 and 2.9%). These results are consistent with the results from dynamic mechanical analysis and can be attributed to improved interfacial adhesion and dispersion of stiff alumina nanowhiskers within the polymeric matrix. By contrast, there was a general trend of a slight decrease in the Young's modulus at increasing raw alumina nanowhisker loading for the blended films.

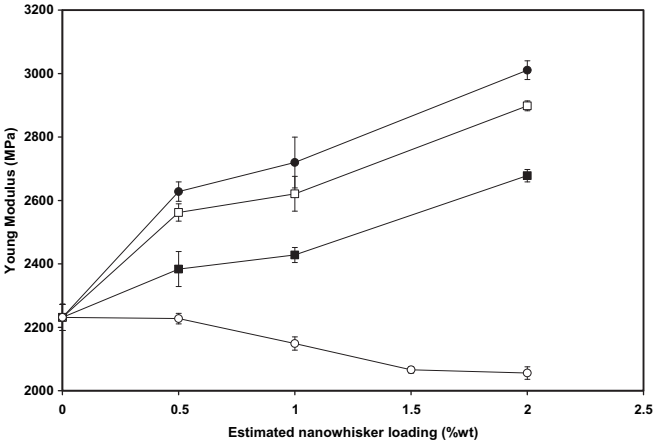

Fig. 6. Young's modulus of the polycarbonate-alumina nanowhisker composites as function of loading of alumina nanowhisker with: (○) PC-R-Al_2O_3, (■) PC-Al_2O_3-RT, (□) PC-Al_2O_3-40, (●) PC-Al_2O_3-55.

There was an initial increase in tensile strength at low raw alumina loading followed by a sharp decrease at higher loading. This increase in tensile strength at low concentration of nanofibers may be due to the formation of fewer agglomerates in the nanocomposite. These agglomerates can act as areas of localized reduced strength and defect sites that result in a general decrease in overall yield strength. Also, the presence of voids near nanowhisker and agglomerate surface could contribute to general decrease in yield strength at higher nanowhiskers loadings.

3.3.2. Nanowhisker dispersion in polycarbonates

The SEM micrographs of the fracture surfaces of the polycarbonate nanocomposites produced with 2 wt% of the raw alumina nanowhisker (PC-R-Al_2O_3-2%) and approximately 2 wt% of the functionalized alumina nanowhisker synthesized at room temperature (i.e. PC-Al_2O_3-RT-2%) are compared in Fig. 8. As discussed in the experimental section, all samples were fractured during the tensile testing at room temperature. Large agglomerates were observed in the composite film made by blending raw alumina nanowhisker in polycarbonate (PC-R-Al_2O_3-2%). This phase separation can be attributed to the poor compatibility of raw alumina nanowhisker with the PC matrix. By contrast, the functionalized alumina nanowhiskers were well dispersed in PC matrix of the PC-Al_2O_3-RT-2%

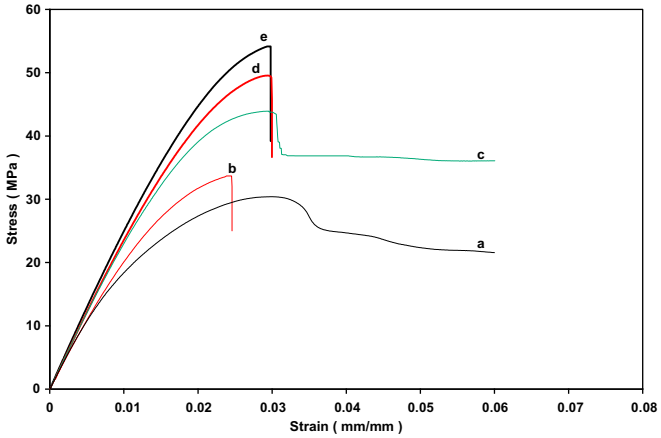

Fig. 5. Samples of stress–strain curve from Instron tensile testing for (a) plain PC, (b) PC-R-Al_2O_3-0.5%, (c) PC-Al_2O_3-RT-0.5%, (d) PC-Al_2O_3-40-0.5%, (e) PC-Al_2O_3-55-0.5%.

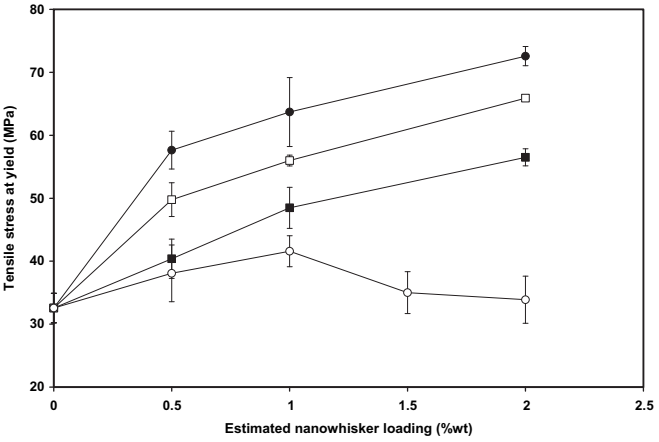

Fig. 7. Tensile strength of the polycarbonate-alumina nanowhisker composites as function of loading of alumina nanowhisker with: (○) PC-R-Al_2O_3, (■) PC-Al_2O_3-RT, (□) PC-Al_2O_3-40, (●) PC-Al_2O_3-55.

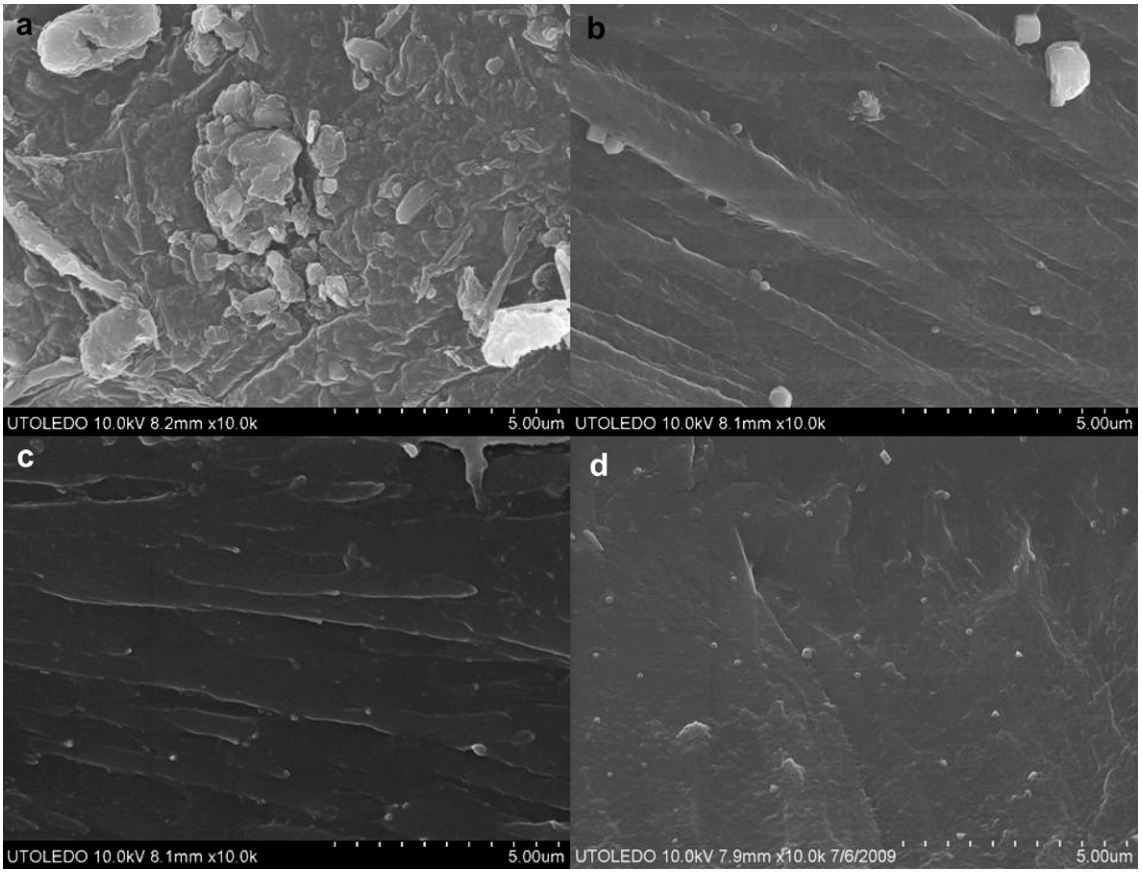

Fig. 8. SEM images of the fracture surfaces for the (a) PC-R-Al_2O_3-2% (scale bar = 5 μm), (b) PC-Al_2O_3-RT-2% (scale bar = 5 μm), (c) PC-Al_2O_3-40-2% (scale bar = 5 μm) and (d) PC-Al_2O_3-55-2% (scale bar = 5 μm). The small white dots in figure are due to the presence of Al_2O_3 nanowhisker.

nanocomposite. While some small particles were visible, no large agglomerates of alumina nanowhisker were observed in the fracture surface. In addition, no gaps were seen at the interface between alumina nanowhisker and PC. Therefore, the PC functionalized alumina nanowhiskers produced using in-situ polymerization and blending with base PC exhibited both good dispersion in the PC matrix and good wetting at the interface between alumina nanowhisker and PC. Similar results were observed by Chandra et al. [25] for fracture surfaces of alumina nanoparticles in PC. This is consistent with high tensile strength seen in tensile testing.

3.3.3. Optical properties

A key goal of this work was to develop transparent polycarbonate nanocomposites with increased strength. The impact of alumina nanowhisker on the optical transparency of the solution cast polycarbonate films was monitored using UV–vis spectroscopy. In addition, digital photos of a picture of the University of Toledo logo were taken with films attached in front of the camera lens, as well as directly on top of the logo. All films used for UV–vis spectroscopy and digital photos have a thickness between 0.15 and 0.16 mm. The resulting photos for the base PC, PC-Al_2O_3-RT at increasing loading and the PC-Al_2O_3-RT-2% are shown in Fig. 9. These photos illustrate that films at 0.5 and 1 wt % loading produced using in-situ polymerization/blending appear to be as clear as the plain PC (see Fig. 9 (a–c)); however, haziness was observed for films of 2 wt% loading. The PC-R-Al_2O_3-2% composite film was unclear and hazy which is consistent with formation of large agglomerates within the composites that can diffract light and/or presence of voids.

The transmittances of the PC nanocomposite films as a function of wavelength are compared with that of plain PC in Fig. 10. The transmittance of the solution cast base polycarbonate is also compared with an extruded plain PC film purchased from McMaster-Carr (Cleveland, OH) to monitor the effect of film production method on optical properties. The extruded film exhibited greater transparency than the solution cast film which is consistent with results reported in literature for polycarbonate [24, 26]. The extruded sample was 0.11 ± 0.01 mm thick. While the PC-Al_2O_3-RT-0.5 wt% exhibited little change in transparency relative to the extruded plain PC film, there was a decrease in transmittance at all wavelengths with increasing alumina loading. The largest impact was seen for transmittance in the UV range at lower wavelengths. A lack of color development was observed in both UV–vis spectroscopy and digital photos. This may be due to the relatively low temperature processing method used to produce the PC-based composites and stability of the alumina nanowhiskers.

As seen in Fig. 10, the PC-R-Al_2O_3-2% composite film was less transparent over most of the wavelength range for visible light. This might be due to the presence of large agglomerates of raw alumina nanowhiskers in the composite film, resulting from poor compatibility with PC matrix. The large aggregated alumina nanowhisker have comparable size to the wavelength of visible light (380–750 nm), which would result in scattering at interface between alumina-rich and polymer-rich phases [17]. It is interesting to note that all PC composites tended to absorb ultraviolet light (<400 nm) much more than pure and extruded plain PC and the absorbance of ultraviolet light of the PC-Al_2O_3-RT composite films significantly increased with increasing loading of alumina nanowhiskers. Zhao et al. [43] saw the same trend for alumina thin films in transmittance data. Therefore, the nanocomposites would have higher UV

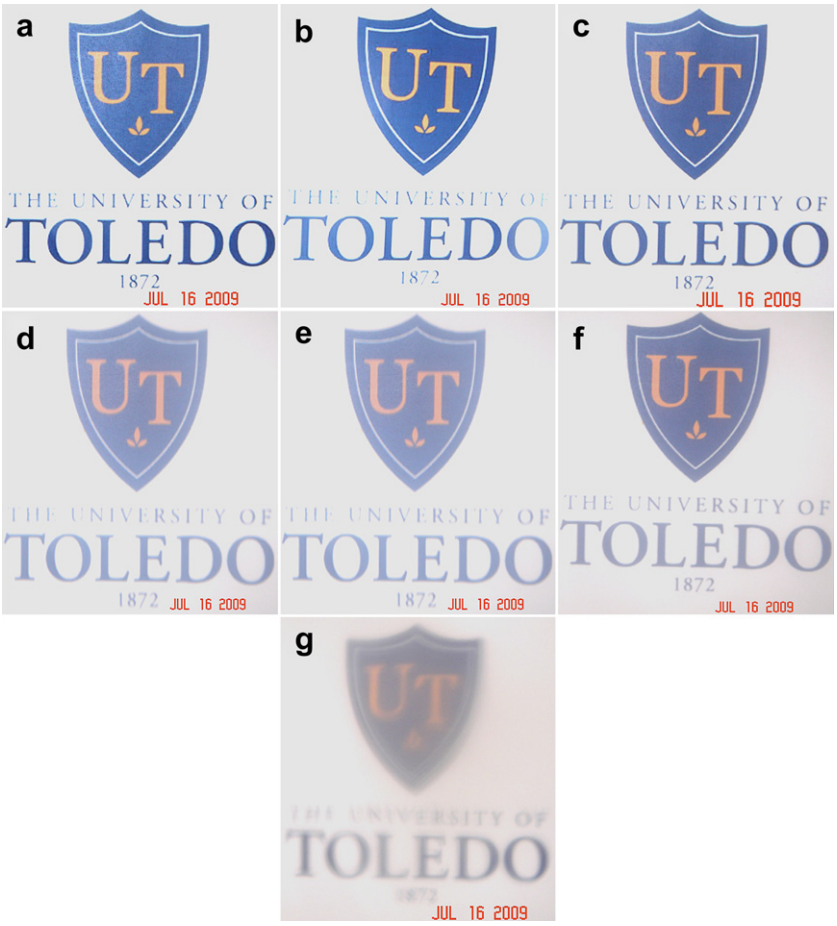

Fig. 9. Digital photos of the (a) plain PC, (b) PC-Al_2O_3-RT-0.5%, (c) PC-Al_2O_3-RT-1%, (d) PC-Al_2O_3-RT-2%, (e) PC-Al_2O_3-40-2% (f) PC-Al_2O_3-55-2% and (g) PC-R-Al_2O_3-2% in front of University of Toledo logo.

protection without significant loss in transparency over the visible range than plain PC.

3.4. Effect of reaction temperature during in-situ polymerization

3.4.1. The tensile properties

The impact of reaction temperature during in-situ polymerization on the mechanical properties of the solution cast composite films is shown in the tensile stress–strain curve for 0.5 wt % fiber loading in Fig. 5. The curve for PC-Al_2O_3-40 shows tensile strength of 49 MPa and strain of 2.9% and the one for PC-Al_2O_3-55 composite has tensile strength of 54 MPa and strain of 2.9%. Therefore, a significant increase in tensile strength was observed with increasing the reaction temperature while the strain remained unchanged. No necking was observed for samples of PC-Al_2O_3-40 and PC-Al_2O_3-55 at all concentrations studied indicating that at high master batch synthesis temperatures, the composite becomes more brittle and does not have a yield point.

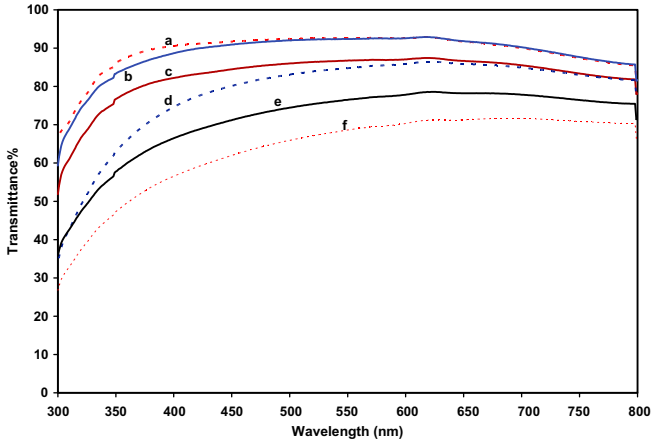

Fig. 10. UV-visible spectra of (a) extruded plain PC, (b) PC-Al_2O_3-RT-0.5%, (c) plain PC, (d) PC-Al_2O_3-RT-1%, (e) PC-Al_2O_3-RT-2%, (f) PC-R-Al_2O_3-2%.

The Young's modulus and the tensile strength of the films made using in-situ polymerization/blending at each reaction temperature are shown as function of loading from 0 to 2 wt% in Figs. 6 and 7. While there is a little change in strain at yield for in-situ polymerized/blended samples, a sharp increase was observed for both Young's modulus and yield tensile stress at elevated reaction temperatures compared to room temperature. For instance, the Young's modulus increased from about 2230–2900 MPa at 40 °C and 3010 MPa at 55 °C for 2 wt %, and the tensile strength from 32 to 66 MPa at 40 °C and 73 MPa at 55 °C. This increase is consistent with the presence of longer oligomeric chain bound to the surface of fiber with increasing reaction temperature which provides improved interaction between the fibers and polymer matrix. In addition, the bulk polymer chain formed during in-situ polymerization at high reaction temperatures has higher molecular weight. This would increase the average molecular weight of the master batch and the resulting blend which would translate to improve properties.

SEM was used to observe the fractured surface following tensile testing of PC-Al_2O_3-RT-2%, PC-Al_2O_3-40-2% and PC-Al_2O_3-55-2% to

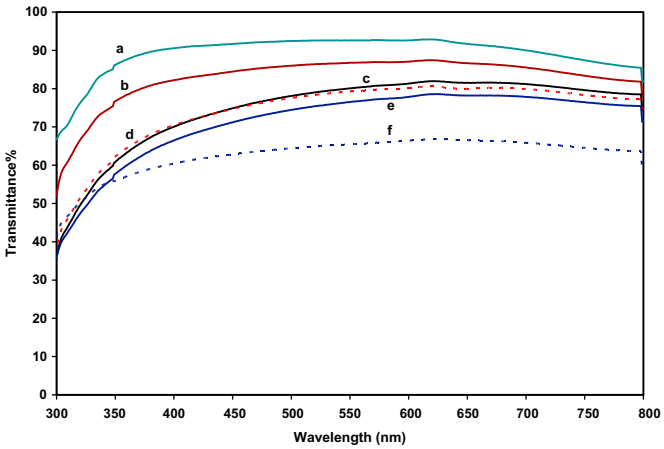

Fig. 11. UV-visible spectra of (a) extruded plain PC, (b) plain PC, (c) PC-Al_2O_3-55-2%, (d) PC-Al_2O_3-40-2%, (e) PC-Al_2O_3-RT-2%, (f) PC-R-Al_2O_3-2%.

monitor the effect of reaction temperature on the dispersion of the nanowhisker in the polymer matrix. The SEM pictures of these composites are compared in Fig. 8. No nanoparticle aggregates were found in the fracture surface for PC-Al_2O_3-40-2% and PC-Al_2O_3-55-2%. In both cases, dispersion of alumina nanowhiskers was very good. Indeed it was hard to observe the presence of nanowhiskers in any of the composites produced using the in-situ polymerization/blending method. This is consistent with presence of higher concentration of polycarbonate on nanofiller surface which would result in improved interfacial wetting and dispersion. (Additionally, wrapping of the nanowhiskers by bulk PC would improve dispersion and mask presence of the nanowhiskers in the SEM images).

3.4.2. Optical properties

The impact of reaction temperature during in-situ polymerization on the optical transparency of the solution cast films was examined using UV–vis spectroscopy. In addition, the digital photos of PC-Al_2O_3-RT-2%, PC-Al_2O_3-40-2%, and PC-Al_2O_3-55-2% over UT logo were taken and shown in Fig. 9. The optical clarity of all films at 2 wt % was similar and comparable to plain PC.

The transmittance of the PC nanocomposite films as a function of wavelength are shown in Fig. 11. The transmittance of the composites at 2 wt % alumina nanowhiskers produced using in-situ polymerization at different temperatures exhibited similar transmittance with slightly higher transparency for master batches produced at higher temperatures. This is consistent with improved dispersion for these samples.

4. Conclusions

Efficient dispersion of alumina nanowhisker in a polycarbonate matrix was achieved using in-situ polymerization to allow covalent bonding PC to the surface of alumina nanowhisker. The highly concentrated nanocomposites formed using in-situ polymerization were diluted with high molecular weight PC to form nanocomposites which exhibited a sharp improvement in mechanical properties (i.e. the Young's modulus and the tensile strength) with little loss in transparency over the whole wavelength range for visible light with respect to pure polycarbonate. Interestingly, these materials also exhibited higher absorbance to the ultraviolet light (<400 nm) than plain PC. The tensile strength and modulus of functionalized alumina nanocomposite at constant nanowhiskers at similar nanowhiskers loadings were higher for samples produced using master batches synthesized at higher temperatures. This was attributed to the growth of polycarbonate chains on the surface of nanowhiskers and higher molecular weight of bulk polymer at higher temperatures that would enhance the interaction between polymer matrix and fibers.

Acknowledgements

The authors would like to acknowledge the US Army Research Office for funding this project with grant number of DAAD 19-03-1-0012. The authors would also gratefully acknowledge Leif Hanson and the InstrumentationCenter at the University of Toledo for use of the Cary 5 Diode Array (HP8452A) UV–vis–NIR spectrophotometer. The Center for Materials and Sensor Characterization at the University of Toledo is also acknowledged for the collection of SEM images.

References

[1] Okamoto M. Journal of Applied Polymer Science 2001;80:2670–5.
[2] Tjong SC, Meng YZ. Journal of Applied Polymer Science 1999;72:501–8.
[3] Tjong SC, Jiang W. Journal of Applied Polymer Science 1999;73:2247–53.
[4] Liaw DJ, Chang P. Journal of Applied Polymer Science 1997;63:195–204.
[5] Dong QX, Chen QJ, Yang W, Zhang YL, Liu X, Li YL, et al. Journal of Applied Polymer Science 2008;109:559–663.
[6] Agarwal S, khan M, Gupta RK. Polymer Engineering and Science 2008;48:2474–81.
[7] Hsieh AJ. Journal of Reinforced Plastic and Composites 2001;20:239–54.
[8] Kayano Y, Keskkula H, Paul DR. Polymer 1998;39:821–34.
[9] Yang YK. Journal of Reinforced Plastics and Composites 2006;25:1279–90.
[10] Jawali ND, Siddaramiah SB, Lee JH. Journal of Reinforced Plastics and Composites 2008;27:313–9.
[11] Sihn S, Kim RY, Huh W, Lee KH, Roy AK. Composites Science and Technology 2008;68:673–83.
[12] Choi YK, Sugimoto KI, Song SM, Endo M. Material Letters 2005;59:3514–20.
[13] Gao Y, He P, Lian J, Wang L, Qian D, Zhao J, et al. Journal of Macromolecular Science 2006;45:671–9.
[14] Eitan A, Fisher FT, Andrews R, Brinson LC, Schadler LS. Composite Science and Technology 2006;66:1159–70.
[15] Sung YT, Kum CK, Lee HS, Byon NS, Yoon HG, Kim WN. Polymer 2005;46:5656–61.
[16] Gao Y, He P, Lian J, Wang L, Qian D, Zhao J, et al. Composites Part A: Applied Science and Manufacturing 2006;37:1270–5.
[17] Zhao Y, Schiraldi DA. Polymer 2005;46:11640–7.
[18] Yoon PJ, Hunter DL, Paul DR. Polymer 2003;44:5323–39.
[19] Yoon PJ, Hunter DL, Paul DR. Polymer 2003;44:5341–54.
[20] Mitsunaga M, Ito Y, Ray SS, Okamoto M, Hironaka K. Macromolecular Material Engineering 2003;288:543–8.
[21] Rama MS, Swaminathan S. Industrial and Engineering Chemistry Research 2010;49:2217–27.
[22] Latella BA, Triani G, Evans P. Journal Scripta Materialia 2007;56:493–6.
[23] Hsieh AJ, Moy P, Beyer FL, Madison P, Napadensky E. Polymer Engineering and Science 2004;44:825–37.
[24] Saarikoski I, Suvanto M, Pakkanen TA. Thin Solid Films 2008;516:8278–81.
[25] Chandra A, Turng L, Gopalan P, Rowell RM, Gong S. Composite Science and Technology 2008;68:768–76.
[26] Hanemann T, Haubelt J, Ritzhaupt-Kleissl E. Microsystem Technology 2009;15:421–7.
[27] Glatkowski, US patent 7, 060, 241, 2006.
[28] Sun J, Gerberich WW, Francis LF. Journal of Polymer Science; Part B 2003;41:1744–61.
[29] Liang GZ, Hu XL, Lu TL. Journal of Materials Science 2005;40:1743–8.
[30] Zeng Z, Yu J, Guo ZX. Macromolecular Chemistry and Physics 2005;206:1558–67.
[31] Gu B, Sen A. Macromolecules 2002;35:8913–6.
[32] Li X, Coleman MR. Carbon 2008;46:1115–25.
[33] Tan CS, Kuo TW. Journal of Applied Polymer Science 2005;98:750–7.
[34] Valmikanathan OP, Ostroverkhova O, Mulla IS, Vijayamohanan K, Atre SV. Polymer 2008;49:3413–8.
[35] Nakayama N, Hayashi T. Progress in Organic Coating 2008;62:274–84.
[36] Higgins BA, Brittain W. J. European Polymer Journal 2005;41:889–93.
[37] Wang J, Gonsalves KE. Journal of Polymer Science: Part A Polymer Chemistry 1999;37:169–78.
[38] Wang J, Montville D, Gonsalves KE. Journal of Applied Polymer Science 1999;72:1851–68.
[39] O'Connell MJ, Boul P, Ericson LM, Huffman C, Wang Y, Haraz E, et al. Chemical Physics Letters 2001;342:265–71.
[40] Tasis D, Tagmatarchis N, Georgakilas V, Prato M. Chemistry – A European Journal 2003;9:4000–8.
[41] Lin T, Bajpai V, Ji T, Dai L. Australian Journal of Chemistry 2003;56:635–51.
[42] Bridgman PW. Studies in large plastic flow and fracture. , New York: McGraw-Hill; 1952.
[43] Zhao ZW, Tay BK, Yu GQ, Chua DHC, Lau SP, Cheah LK. Thin Solid Films 2004;447–448:14–9.